RL-TR-94-186
In-House Report
November 1994

ADVANCED PRESORT PROCESSOR

David Grucza

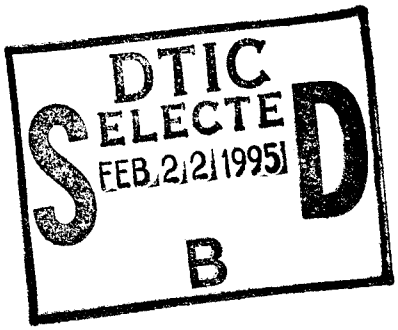

APPROVED FOR PUBLIC RELEASE; DISTRIBUTION UNLIMITED.

Rome Laboratory
Air Force Materiel Command
Griffiss Air Force Base, New York

This report has been reviewed by the Rome Laboratory Public Affairs Office (PA) and is releasable to the National Technical Information Service (NTIS). At NTIS it will be releasable to the general public, including foreign nations.

RL-TR-94-186 has been reviewed and is approved for publication.

APPROVED: James W. Cusack

JAMES W. CUSACK, Chief
Photonics & Optics Division
Surveillance & Photonics Directorate

FOR THE COMMANDER: Donald W. Hanson

DONALD W. HANSON
Director of Surveillance & Photonics

If your address has changed or if you wish to be removed from the Rome Laboratory mailing list, or if the addressee is no longer employed by your organization, please notify RL (OCPA) Griffiss AFB NY 13441. This will assist us in maintaining a current mailing list.

Do not return copies of this report unless contractual obligations or notices on a specific document require that it be returned.

REPORT DOCUMENTATION PAGE

Form Approved
OMB No. 0704-0188

1. AGENCY USE ONLY (Leave Blank)	2. REPORT DATE	3. REPORT TYPE AND DATES COVERED
	November 1994	In-House Dec 91 - Sep 93

4. TITLE AND SUBTITLE
ADVANCED PRESORT PROCESSOR

5. FUNDING NUMBERS
PE - 62702F
PR - 4600
TA - P1
WU - 12

6. AUTHOR(S)
David Grucza

7. PERFORMING ORGANIZATION NAME(S) AND ADDRESS(ES)
Rome Laboratory (OCPA)
25 Electronic Pky
Griffiss AFB NY 13441-4515

8. PERFORMING ORGANIZATION REPORT NUMBER
RL-TR-94-186

9. SPONSORING/MONITORING AGENCY NAME(S) AND ADDRESS(ES)
Rome Laboratory (OCPA)
25 Electronic Pky
Griffiss AFB NY 13441-4515

10. SPONSORING/MONITORING AGENCY REPORT NUMBER

11. SUPPLEMENTARY NOTES
Rome Laboratory Project Engineer: David Grucza/OCPA (315) 330-2105

12a. DISTRIBUTION/AVAILABILITY STATEMENT
Approved for public release; distribution unlimited.

12b. DISTRIBUTION CODE

13. ABSTRACT (Maximum 200 words)

The purpose of the Presort Processor is to excise strong narrow band signals from a wideband radar return. It is an optical notch filter based on acoustooptics and fourier transform optics. This latest iteration of this project uses a narrow bandwidth doubled Nd:YAG laser as an optical carrier and a TIR (total internal reflection) liquid crystal spatial light modulator to perform the frequency excision.

14. SUBJECT TERMS optical notch filter, acoustooptics, fourier transform optics, TIR (total internal reflection), liquid crystal spatial light modulator, frequency excision

15. NUMBER OF PAGES 36

16. PRICE CODE

17. SECURITY CLASSIFICATION OF REPORT	18. SECURITY CLASSIFICATION OF THIS PAGE	19. SECURITY CLASSIFICATION OF ABSTRACT	20. LIMITATION OF ABSTRACT
UNCLASSIFIED	UNCLASSIFIED	UNCLASSIFIED	U/L

Table of Contents

1. Introduction:

The purpose of the Presort Processor is to excise strong narrow band signals from a wideband radar return. It is an optical notch filter based on acoustooptics and fourier transform optics, both of which are briefly explained in the theory section of this report.

A notch filter of this type was built by Harris Corporation[1] for RL. The goal of this project is to build a new notch filter using components which have been improved in the years since Harris first designed and built the original Presort Processor.

The components to be replaced are the laser, which provides an optical carrier, and the spatial light modulators, which block selected portions of the modulated optical carrier to produce notches in the RF output. The 830 nm laser diode used by Harris were replaced with a 532 nm doubled Nd:YAG, the Nd:YAG offering more stability and power. The acoustooptic spatial light modulators were replaced by a TIR (total internal reflection[2]) cell which is more compact, requires lower drive power, and gives better optical extinction.

2. Theory:

2.1 Introduction

The presort processor is based on the ability of an acoustooptic cell to both frequency shift a laser beam by an input radio frequency and to direct this shifted light in a unique direction. The first property allows the use of a laser beam as an optical frequency carrier with the cell acting as the frequency modulator. The second property causes the various frequencies in the modulated laser carrier to be spread out in space (see section 2.3). Filtering is performed by blocking whichever frequencies we wish to get rid of (blocking part of the light coming out of the acoustooptic cell). After this "spatial filtering" the signal on the optical carrier can be taken down to the original band of radio frequencies by beating against an optical reference that was split off of the laser source which supplied the optical carrier(see section 2.4).

Referring to figure 2.1.1: C1 ,C2 ,C3, and C4 collimate the beam in the plane of the drawing and focus the beam into the aperture of the acoustooptic cell. This is shown in more detail in figure 2.1.2. BS1 splits half the power off of the laser beam for use as a local oscillator reference. The purpose of I1 is to bring the reference beam to a focus at the photodetector. As shown in figure 2.1.3, I1 is positioned so that the point where the reference beam comes to a focus and the center of the Bragg Cell are the same distance from the beam combiner(BS2). The optics in the remainder of the system will image anything at this point, onto the photodetector. Thus, the Bragg Cell aperture and the apparent point source both form images at the detector. The Bragg Cell acts as a frequency modulator as will be explained in Section 2.2. For this system the input radio frequency signal to be filtered (notched) is located between 250 Mhz and 450 Mhz. BS2 acts to combine the frequency modulated optical carrier with the reference. The diffracted frequency shifted light is fourier transformed by the lenses labeled F1, F3, and F4, the transform plane falling at the center of the liquid crystal spatial light modulator. In figure 2.1.4, the diffracted beam shown corresponds to an input frequency of 350 MHz. F2 focuses the light into the plane of the spatial light modulator. The spatial light modulator implements the desired filtering by blocking light corresponding to the unwanted frequency bands. It is a 200 channel TIR[3] cell which deflects undesired

signals away the photoreceiver (out of the page). Its operation is covered in section 2.5. C1 collects the filtered light and focuses it onto the photodetector. The filtered signal is recovered by optical heterodyning with the reference beam that copropagates with the signal beam from the interferometer's output beam splitter cube(BS2).

The shape of the notch in the spectrum of the filtered output depends on the depth of focus and spot size of the transform of the diffracted light with respect to the TIR channel dimensions. If the light deflected at the Bragg Cell corresponding to a given signal frequency is spread over a number of spatial channels, turning off one channel will remove only a small part of the signal from the output and will result in a wide, shallow notch. If, however, the light from a given frequency is focused through a single channel, turning off the channel will completely remove that frequency from the output and will result in a steep narrow notch.

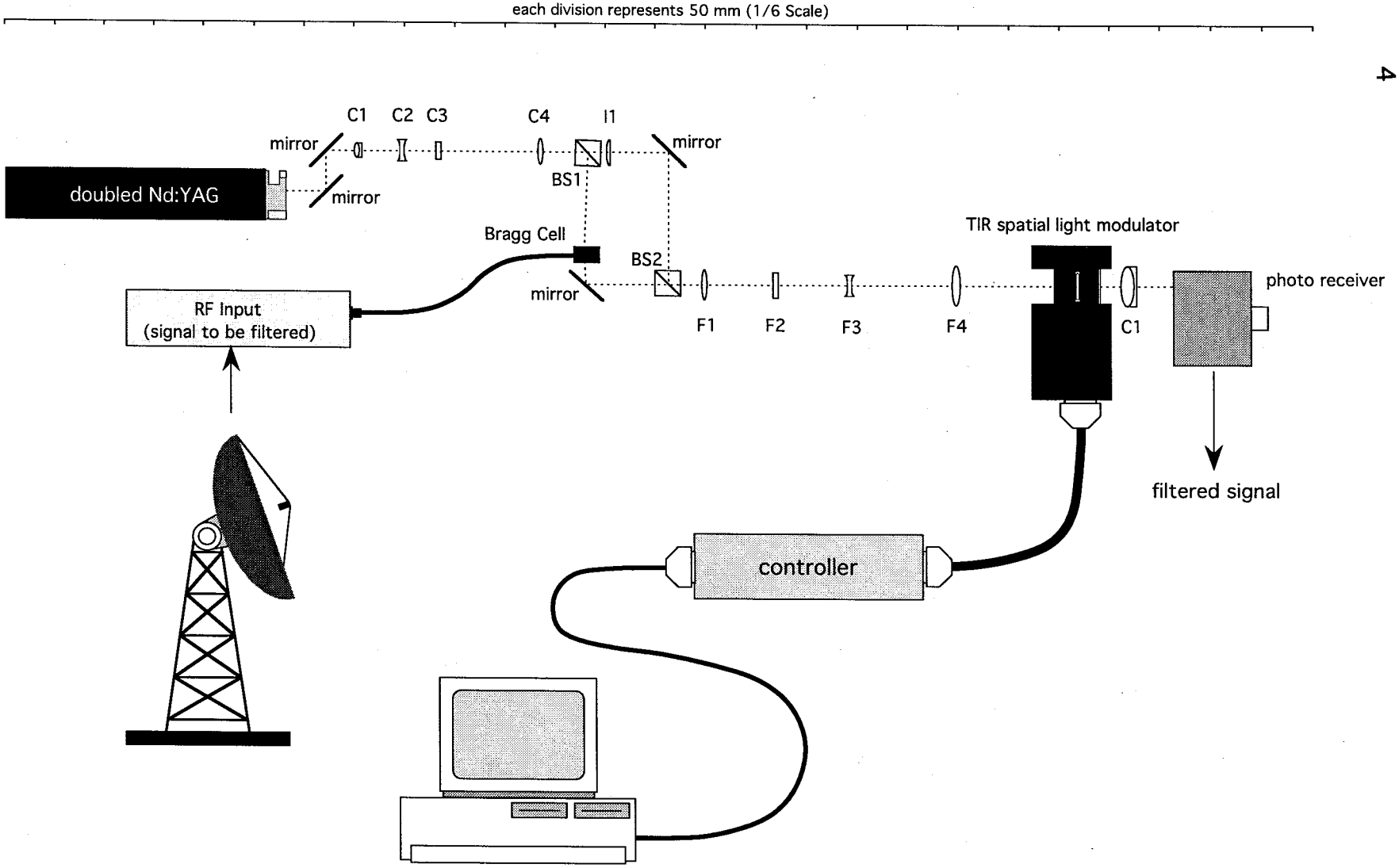

Figure 2.1.1: Optics Layout

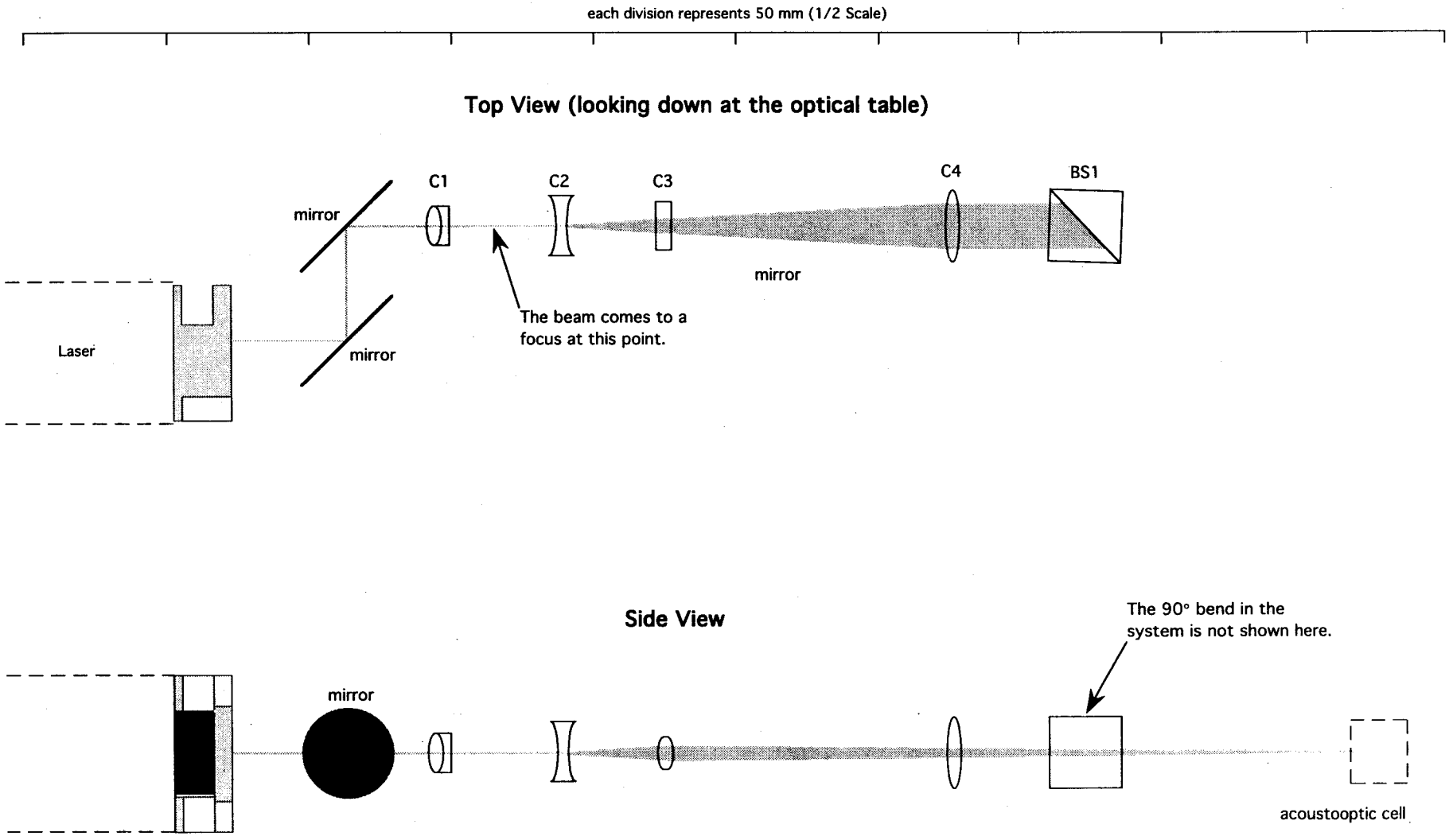

Figure 2.1.2: Collimating Optics

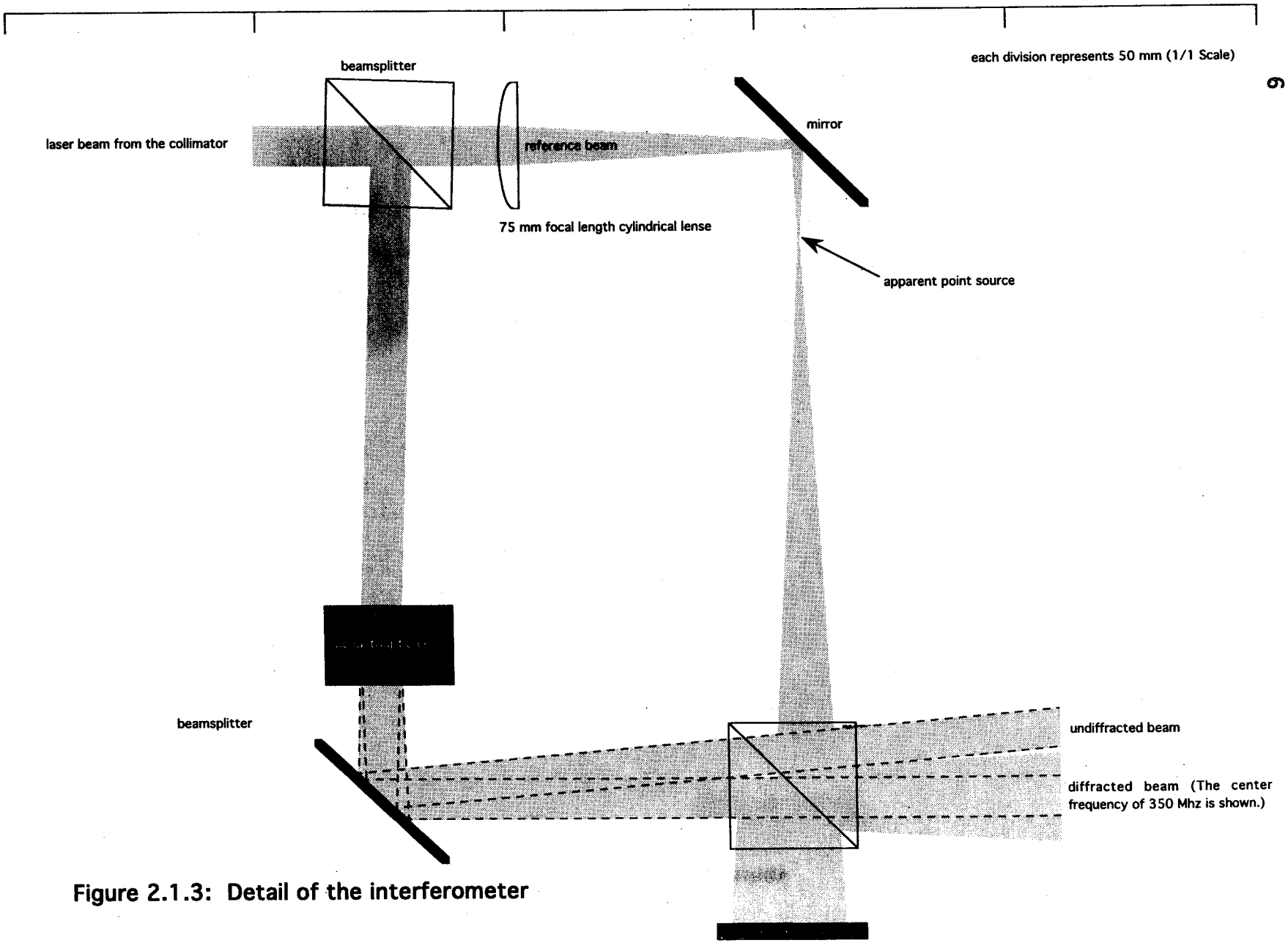

Figure 2.1.3: Detail of the interferometer

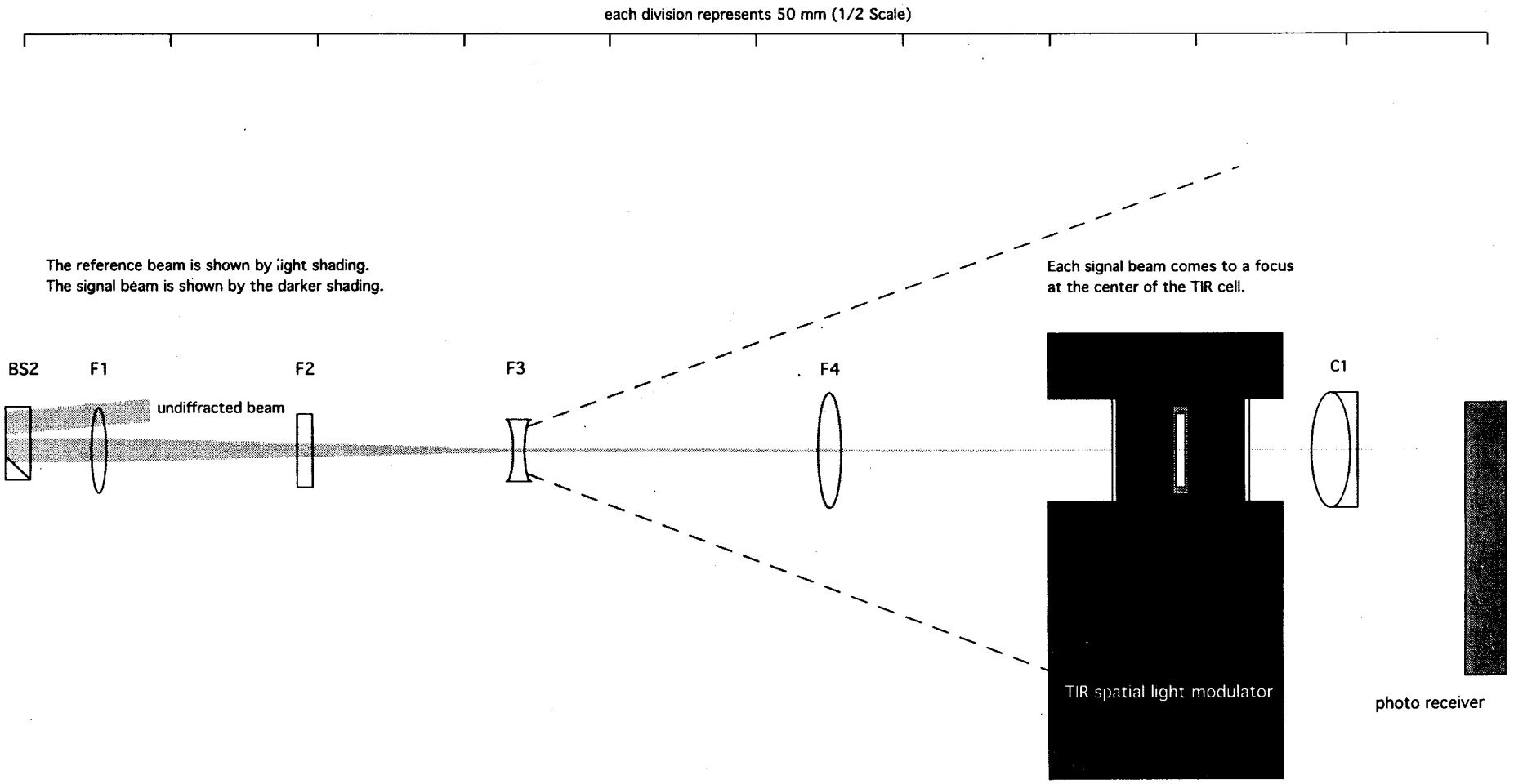

Figure 2.1.4: Detail of the transform and the collection optics.

2.2 Acoustooptic Diffraction

An acoustooptic cell is a device commonly used to deflect(to steer) a laser beam. As pictured below, it consists of a block of glass (or a crystalline material) with piezoelectric transducers affixed to one endface. The transducers are driven by an RF signal, setting up acoustic compression waves in the crystal which act as a diffraction grating. When a laser beam is directed through these compression waves light will be diffracted if it is incident on the acoustic waves at the correct angle, labeled θ in Figure 2.2.1. This is referred to as the Bragg Angle, and for light incident at this angle reflections occurring throughout the crystal add up constructively to give a diffracted beam.

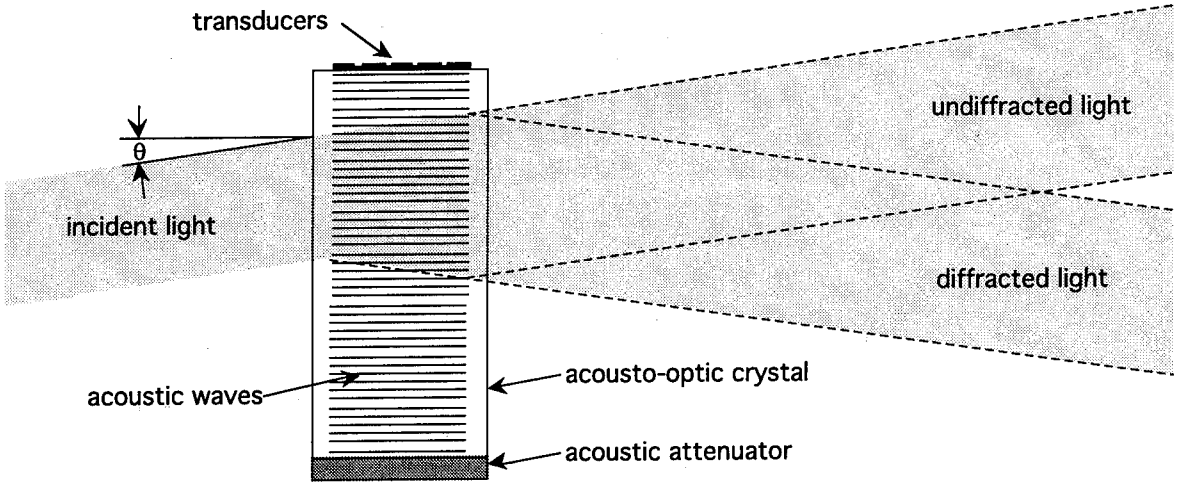

Figure 2.2.1: Acoustooptic Cell

To see this, first consider figure 2.2.2, which shows the reflection of light incident on a partially reflecting mirror at incidence angle θ. The parallel dotted lines indicate the orientation or the optical wavefronts. To approximate the acoustic wave in the crystal, a number of partially reflecting mirrors can be placed parallel to one another spaced one acoustic wavelength apart, as pictured in figure 2.2.3. Here, the superimposed reflections do not add constructively, as can be seen by the misalignment of the reflected optical wavefronts. By leaving the optical and acoustic wavelengths unchanged and adjusting the angle, the reflected

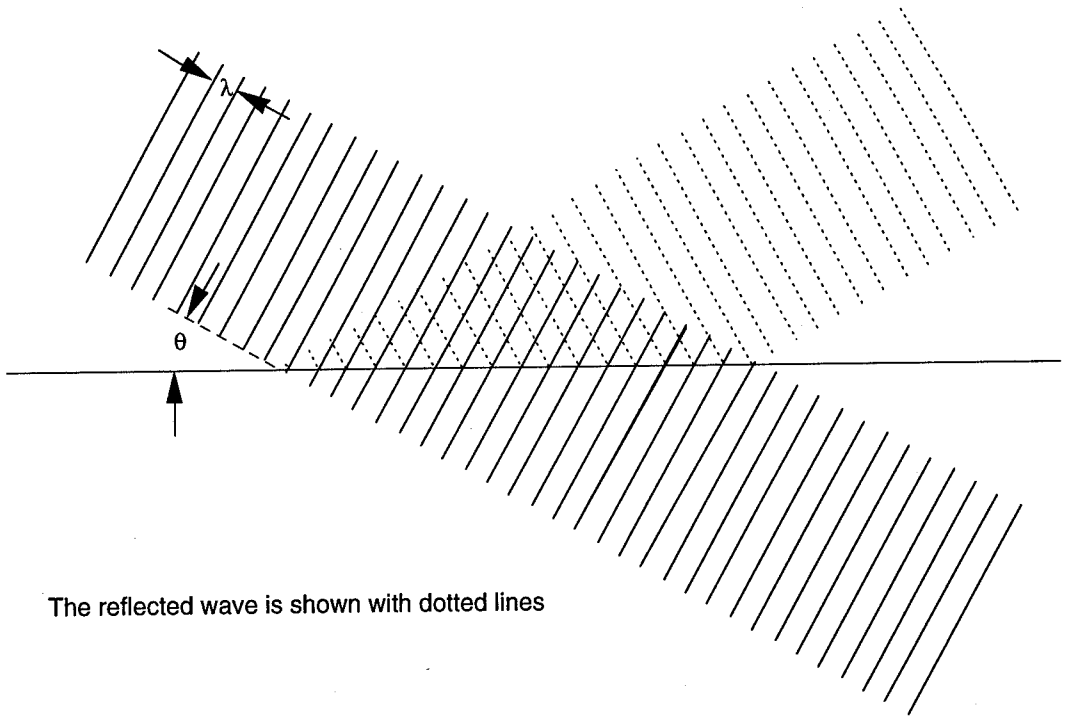

Figure 2.2.2: Reflection of light from a partially reflecting mirror at angle θ.

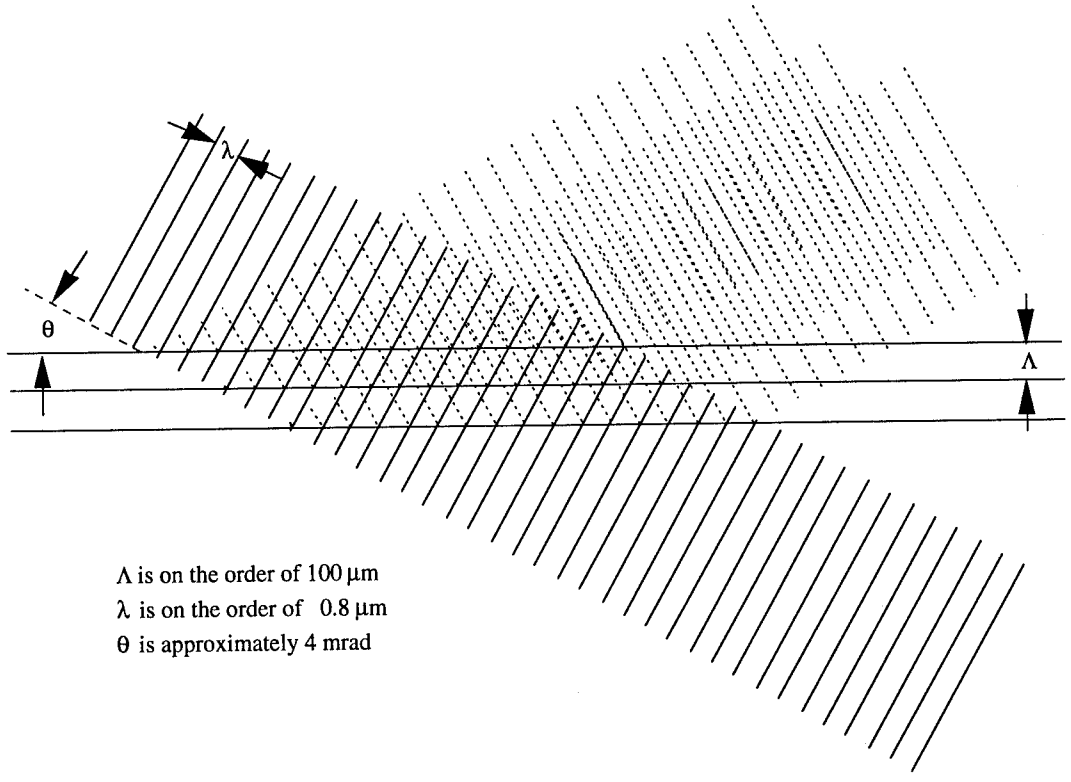

Figure 2.2.3: Reflection from a periodic structure of partially reflecting mirrors. The Bragg condition is not satisfied.

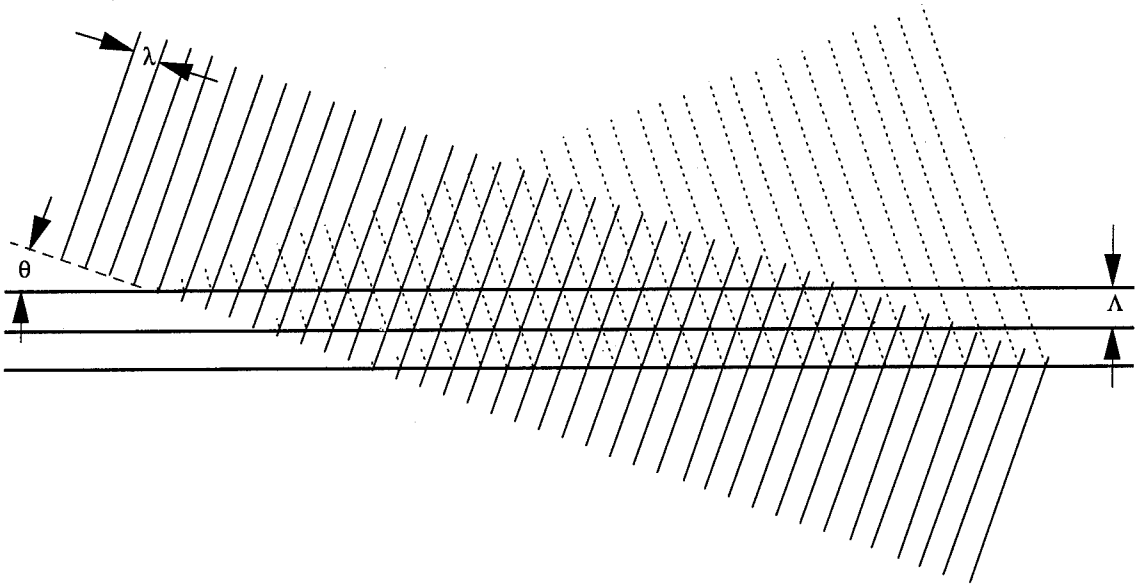

Figure 2.2.4: Bragg diffraction condition is satisfied.

wavefronts are brought into alignment to interfere constructively as in figure 2.2.4, giving a diffracted beam.

The above explanation is a bit superficial in that interference of the reflections somewhere away from the mirrors doesn't matter, but it does lead to the correct answer. It is the phase of all of the partial reflections at the partially reflecting mirrors that leads to boundary conditions that will produce a reflected beam.

Also, in these figures the wavefronts were considered to be stationary. For moving wavefronts, as in the acoustooptic cell, the diffracted waves will be Doppler shifted by the acoustic frequency causing the diffraction. This will be an upshift if the incoming light is pointed more towards the transducer, and a downshift if pointed more away from the transducer. This frequency shifted light is what carries the signal in the Presort. Heterodyning of this light with unshifted light gives the Presort's output, as explained in section 2.4.

2.3 Acoustooptic Spectrum Analysis and Notch Filtering

The Presort Processor is based on the technique of acoustooptic spectrum analysis, which utilizes the characteristic of a Bragg Cell to deflect light at an angle proportional to the acoustic frequency propagating through the cell.

Figure 2.3.1 shows two such diffracted beams which would result if a signal consisting of two frequencies, such as a double sideband suppressed carrier, were fed into the cell. Let these be 340 Mhz and 360 Mhz. As shown in figure 2.3.1, a lens will focus these diffracted beams to two different points because they enter the Fourier Transform Lens at differing angles. The intensity of each point of light will correspond to the strength of each frequency component in the RF input signal. In this way, all differing frequencies are mapped to a point of light at an intensity proportional to the their amplitudes. By scanning across the focal plane (in this case a line) and noting the intensity of the light at each position, we can obtain the RF spectrum of the input signal. The focal plane is referred to as the Fourier Transform Plane.

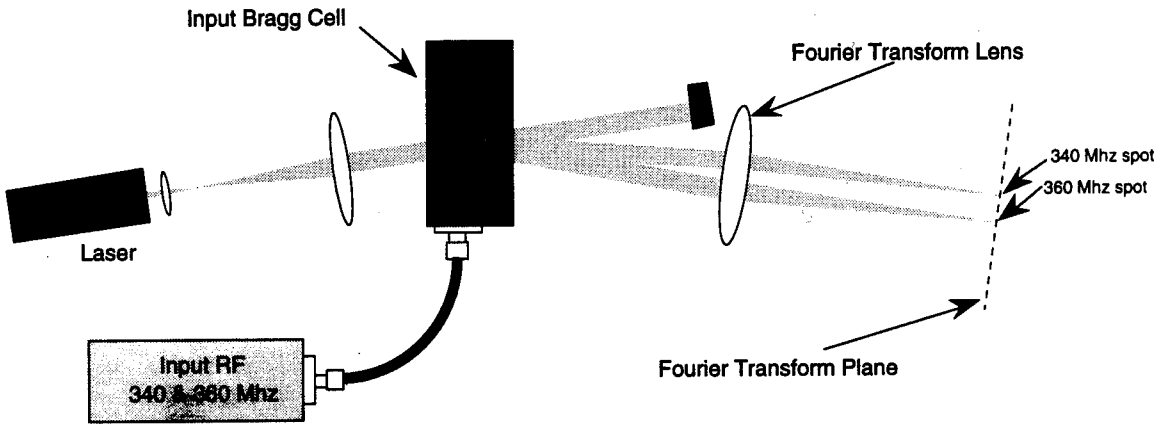

Figure 2.3.1: Acoustooptic Spectrum Analysis

As stated in section 2.2, each of the beams is Doppler Shifted in frequency by the frequency component that produced it. If these beams are imaged onto a detector with an unshifted beam of light, they will interfere (heterodyne) to reproduce the original signal at the detector output. If either of the frequency shifted beams is blocked from reaching the detector, its corresponding frequency will not be present in the photodetector output. The beams can be blocked independently of each other in the Fourier Transform Plane. This is where the TIR cells(spatial

light modulators) are placed in the Presort.

The Bragg matching condition is maintained over the range of input frequencies by using a phased array transducer. The phased array causes differing acoustic frequencies to propagate at differing angles to the axis of the Bragg Cell, and thus at the appropriate angle to the input light beam.

The actual angular range over which light is deflected is only 12 mrad or 0.69° as calculated below. This small angle must be spread out over the entire spatial light modulator by use of magnifaction optics so that it may be filtered.

The equation for the Bragg deflection angle (α_B) is:

$$\alpha_B = \sin^{-1}\left\{\frac{\lambda}{\Lambda}\right\} = \sin^{-1}\left\{\frac{\lambda f}{2v}\right\}$$

where α_B is the deflection angle

λ is the optical wavelength (532 nm)

Λ is the acoustic wavelength

v is the acoustic velocity ($4.2 \times 10^3 \ \frac{m}{s}$)

f is the acoustic frequency (2.5×10^8 hz to 4.5×10^8 hz)

The minimum deflection angle is:

$$\alpha_{B(min)} = \sin^{-1}\left\{\frac{5.32 \times 10^{-3}\ m \cdot 2.5 \times 10^8\ \frac{1}{s}}{2 \cdot 4.2 \times 10^3\ \frac{m}{s}}\right\} = 0.91° = 16\ \text{mrad}$$

The maximum deflection angle is:

$$\alpha_{B(max)} = \sin^{-1}\left\{\frac{5.32 \times 10^{-3}\ m \cdot 4.5 \times 10^8\ \frac{1}{s}}{2 \cdot 4.2 \times 10^3\ \frac{m}{s}}\right\} = 1.6° = 28\ \text{mrad}$$

The deflection range is 12 mrad, the difference between the maximum and minimum deflection angles.

2.4 Optical Heterodyne Detection

This section briefly treats the recombination and beating together of the signal beam and the reference beam at the photodetector that produces the Presort's output signal. This also shows the need for I1(the cylindrical lens) in the interferometer reference leg of figure 2.1.1.

At the photodetector, the various diffracted beams, corresponding to the frequencies present in the input signal, combine to form an image of the Bragg Cell aperture. Each beam forms a complete image of the aperture. They overlap as shown in figure 2.4.1. Each of these beams strike the photodetector at differing angles. This is also shown in figure 2.4.2 for two differing diffracted beams, represented by the plane wavefronts entering the detector.

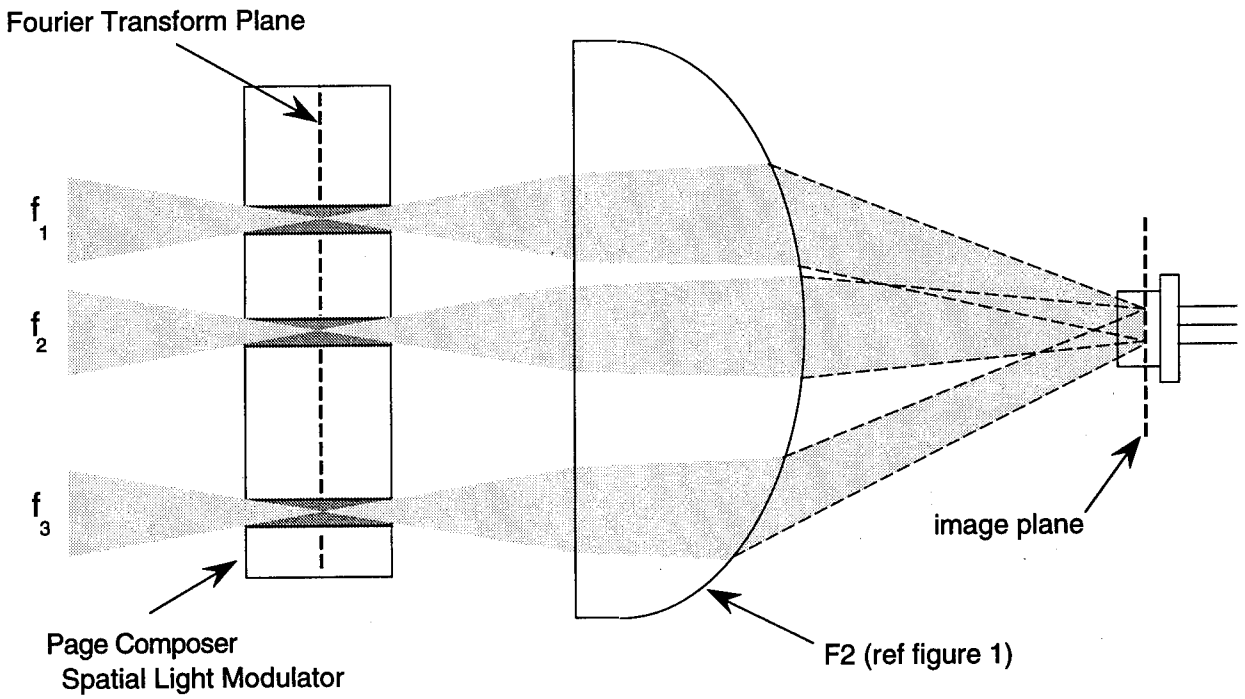

Figure 2.4.1: Formation of an image of the Bragg Cell aperture.

In beating together two signals to get the difference frequency, the alignment of the beams determines how much the wavefronts overlap, and thus, the strength of the difference signal. To beat equally with each

signal beam, and produce a flat system frequency response, the reference beam must come to a focus at the photodetector. This converging reference beam is shown by the curved wavefronts of figure 2.4.2. The shaded areas in the figure indicate where there is sufficient alignment of the wavefronts to produce a signal as they beat together.

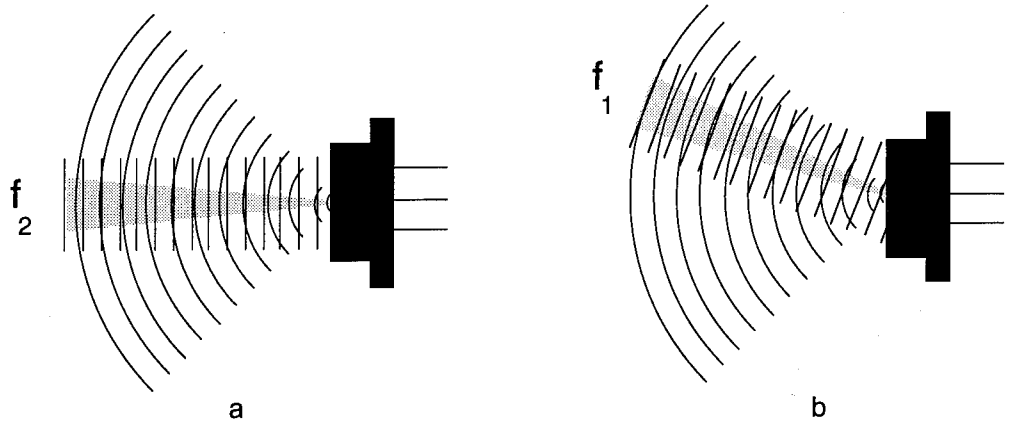

Figure 2.4.2: Sampling of acoustooptic aperture by heterodyne detection.

As explained in section 2.1, the converging reference beam is produced by the cylindrical lens(l1) in the reference leg of the interferometer.

Note: The signal beams do not strike the detector as collimated beams in the actual system. They are shown in this manner for clarity.
This process can also be viewed as an interferometric modulator because the reference beam and various frequency components of the signal beam running in and out of phase with each other at the output beamsplitter cause optical power to be shifted from one output leg to the other at the RF frequencies present in the input signal. The photodetector then recovers the envelope of the light frequency carrier.

2.5 DisplayTech TIR(total internal reflection) Cell

A full size drawing of the TIR spatial light modulator is shown in figure 2.5.1. The cutaway view at the top of the drawing shows the glass prisms and the path taken by the light through the modulator. Two exit beams are shown, a deflected beam (corresponding to a notch in the Presort's output) and a beam going straight through (corresponding to frequencies that are present in the output). Figure 2.5.2 shows a progressive blowup of the active area, each pixel being 0.120" long and 123 μm wide with a dead space of 2 μm between the pixels. The lower drawing shows an outline of the modulator and the location of the active area within the glass prisms. The first blowup shows portions of the linear array with pixels drawn proportionally. The second blowup shows the gap between the pixels.

The cell is based on the principle of total internal reflection[4] which is illustrated in figure 2.5.3. When light is incident upon an interface between two different materials (in this case the materials are the glass and the liquid crystal film) at a grazing angle it can be completely reflected for certain values of the indices of refraction of the materials. The liquid crystal has different values of the index of refraction for s-polarized and p-polarized light. For these modulators p-polarized light always undergoes total internal reflection and cannot be used with the TIR cell, so only s-polarized light is considered in what follows. The index of refraction depends on the orientation of the liquid crystal's molecules as shown by the enlargements of the active area in the figure. In the On State the alignment of the liquid crystal gives an index of refraction equal to that of the glass, and effectively eliminates the glass-liquid crystal interface. In the Off State the index of refraction of the liquid crystal is such as to cause a total internal reflection of the incident light[5]

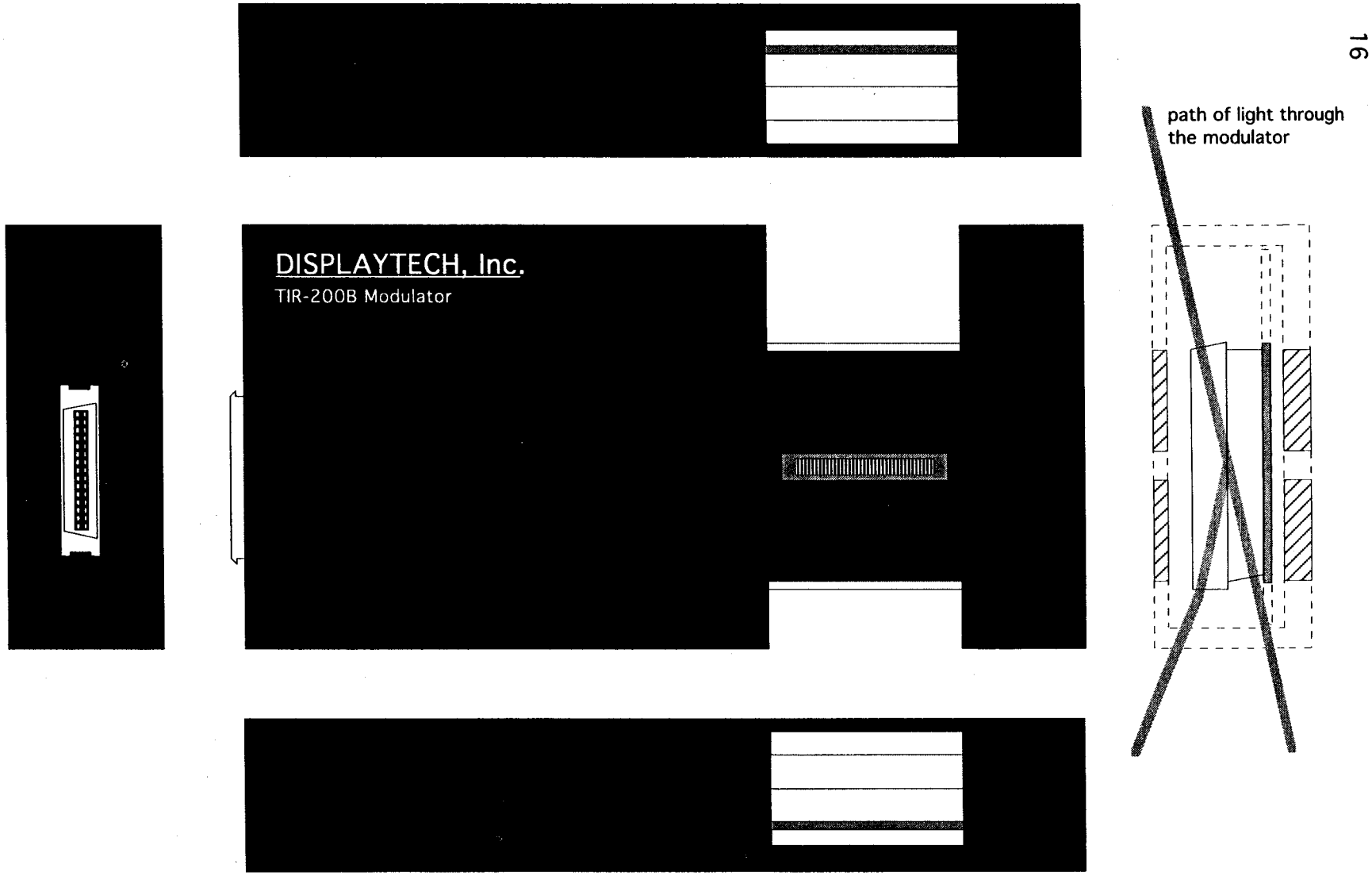

Figure 2.5.1: 1:1 Scale drawing of the DisplayTech TIR cell

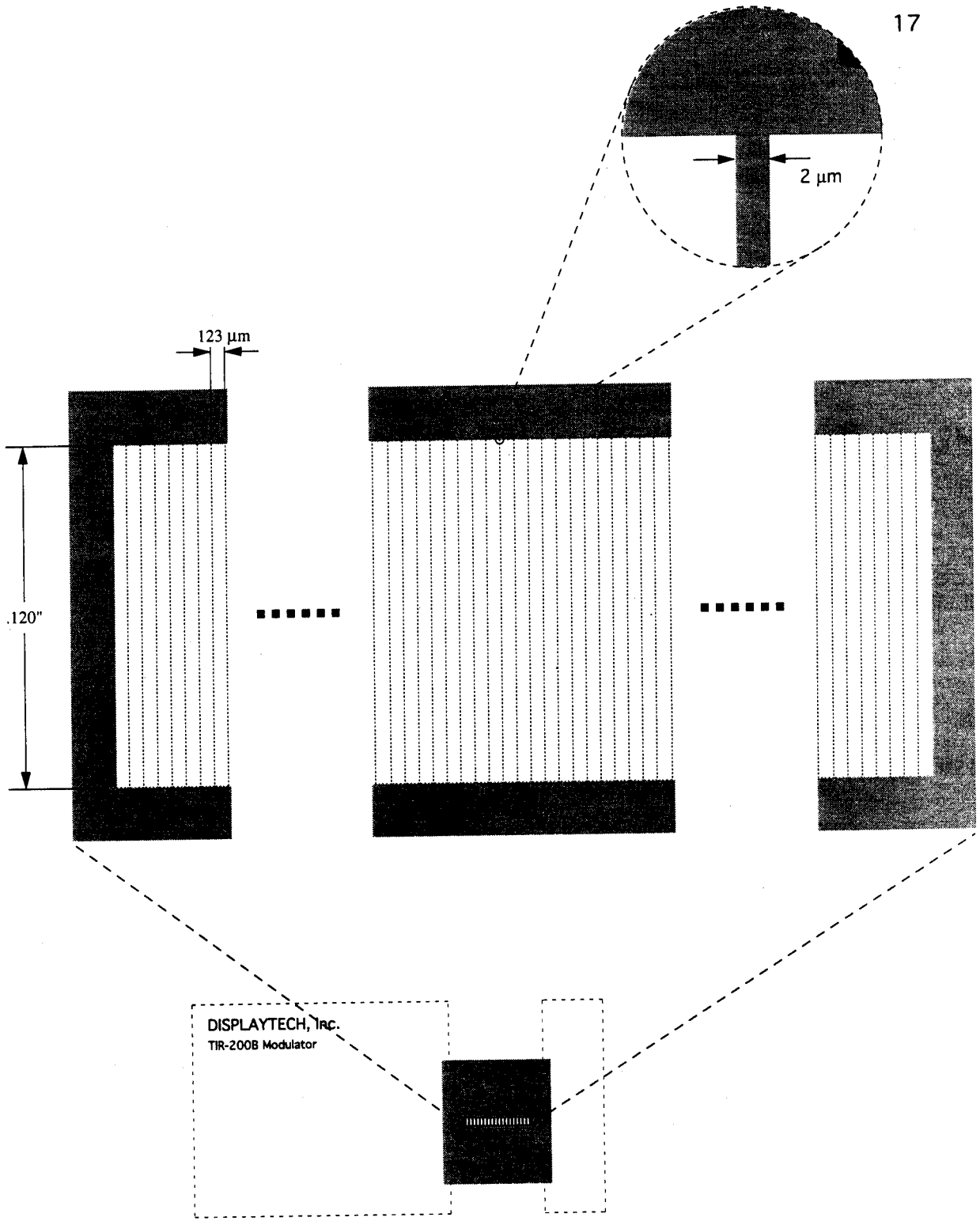

Figure 2.5.2: Pixel arrangement of the TIR SLM

Figure 2.5.3:
TIR (total internal reflection) Liquid Crystal Spatial Light Modulator

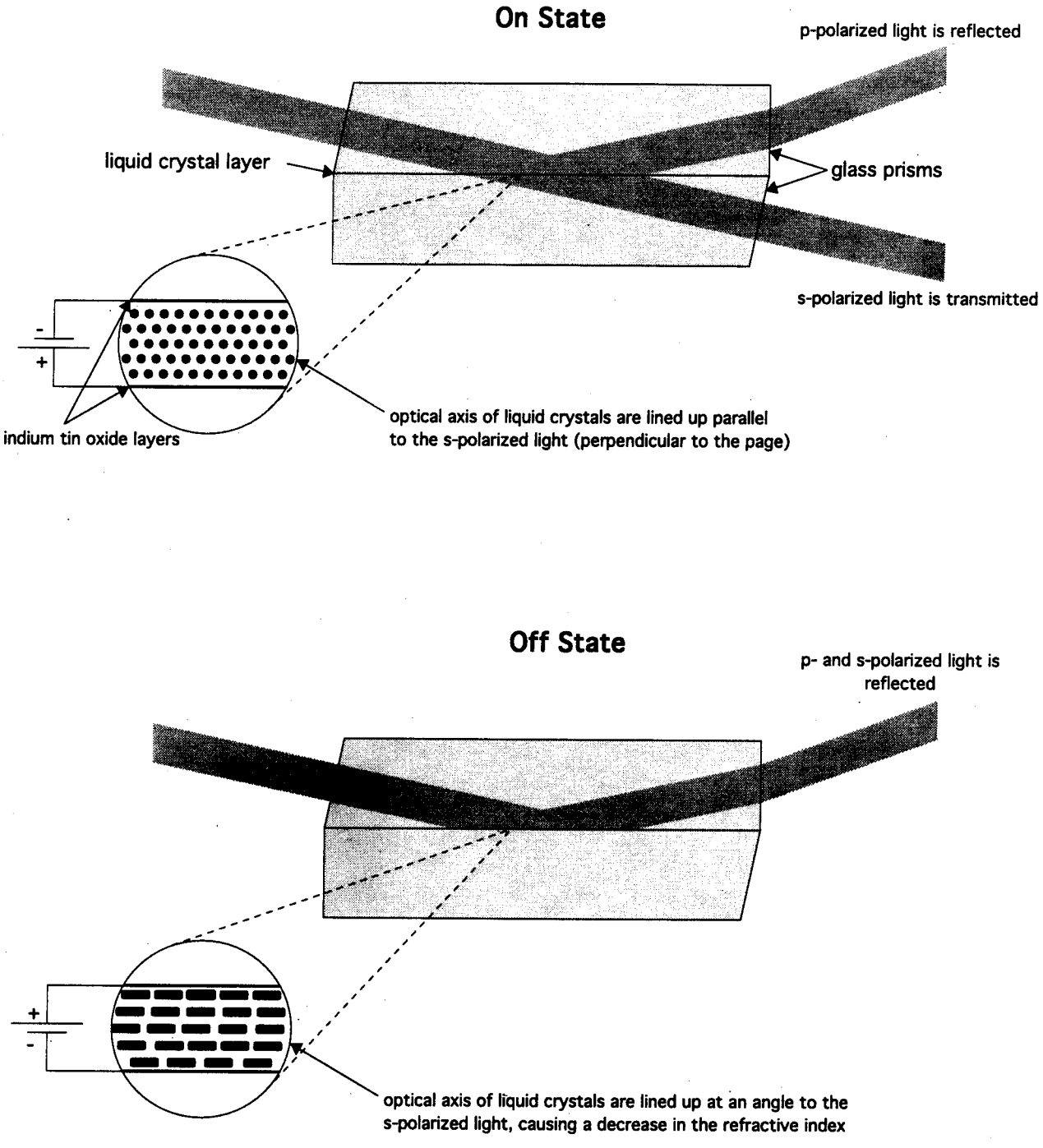

3. Observations and Results:

The system transfer function and noise floor are shown in Figure 3.1. From this graph, the system dynamic range is 69 dB into a 3 kHz bandwidth. Using the real system bandwidth of 200 MHz rather than the 3 kHz resolution bandwidth of the network analyzer lowers the dynamic range by 48 dB, giving an operational dynamic range of 21 dB. This could be improved by approximately 10 dB with the addition of shielding, especially between the acoustooptic cell (which acts as an antenna) and the photoreceiver. The passband could also be flattened by use of a different acoustooptic cell, the rolloff at the higher frequencies being caused by a loss of response in the cell at these frequencies.

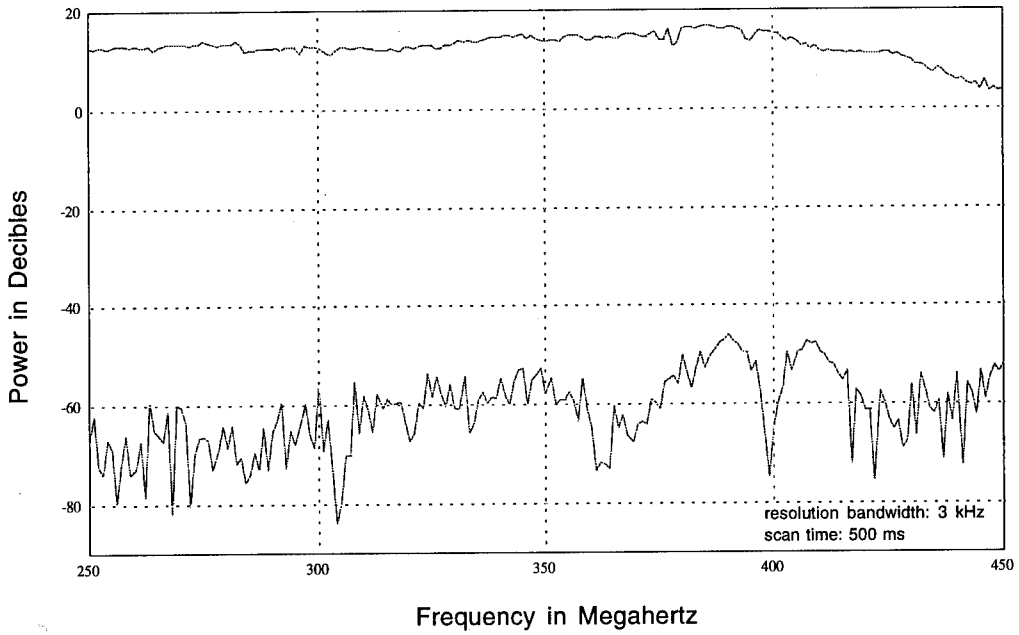

Figure 3.1: The system transfer function is shown by the upper trace, the noise floor by the lower trace.

A single notch at the system center frequency is shown in Figure 3.2. It is very irregular and is 12 dB deep, only half of what it should be. The reason for this poor performance is a somewhat irregular focus in the Fourier Plane. There is a Gaussian main focus spot 115 μm wide with a small sidelobe 40 μm wide. One channel on the SLM is 125 μm wide, and is not sufficient to eliminate all of a 1 MHz bandwidth signal. Because of

the poor focus, multichannel notches are much deeper, but tend to be very narrow. As can be seen in Figure 3.3 a 2 MHz notch is 47 dB deep as is the 3 MHz notch shown in Figure 3.4.

This poor performance is the result of an attempt to greatly shorten the optical train of the system, especially that of the Fourier Transform Optics. The optics are somewhat more complicated than necessary. The size of the optics was also made fairly small, inch diameter optics or smaller were used in place of optics measuring greater than two inches in diameter on the original system. This resulted in truncation of the beam.

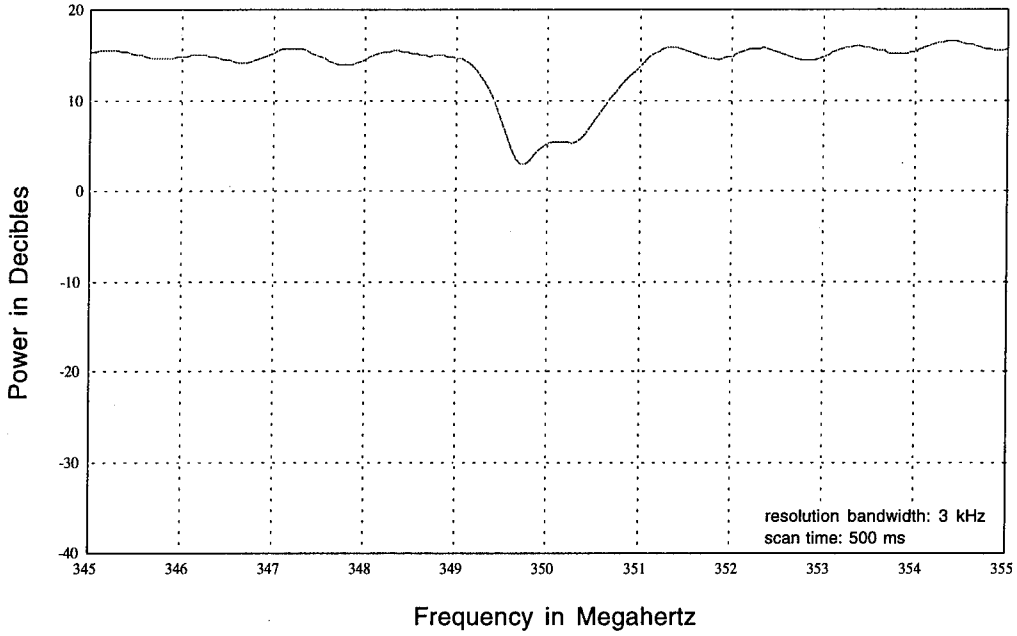

Figure 3.2: The system transfer function with a single notch at 350 MHz.

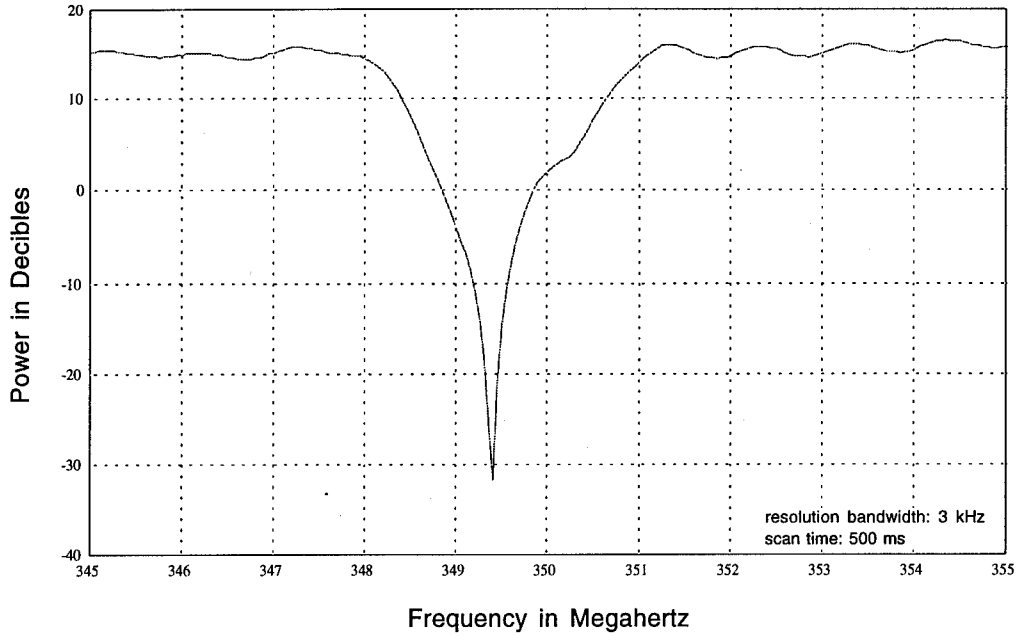

Figure 3.3: The system transfer function with two adjacent notches, at 349 MHz and at 350 MHz.

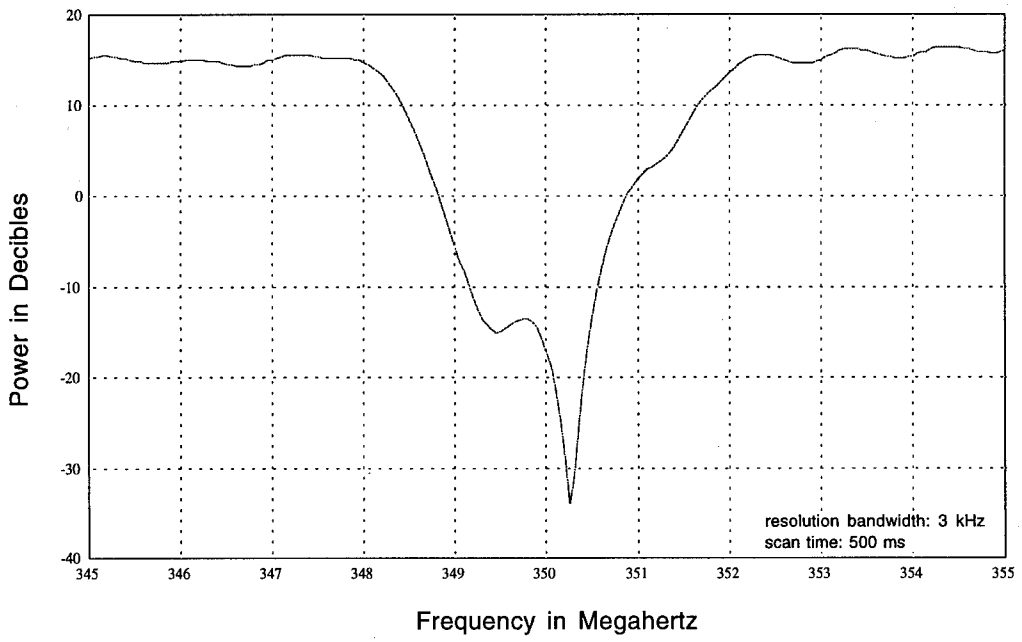

Figure 3.4: The system transfer function with three adjacent notches, at 349 MHz, 350 Mhz, and 351 MHz.

4. Conclusions:

The system did not perform as desired. The frequency notches tended to be irregular and very narrow. The depth of the notches shows that the TIR liquid crystal modulator is very effective however.

I believe that if much more attention is given to the optical design the performance goals for this processor can be met. Antireflection coating of the optics would greatly increase the signal strength. Currently, only about 5 mW of optical power is reaching the photodetector. This would increase to about 18 mW with the coated optics. Computer modeling of the optics, taking into account aberrations due to the short focal length optics used and beam truncation because of the small diameters of the optics, will result in a better focus in the Fourier Plane. It might be necessary to go to slightly larger optics and to increase the length of the system. But doing so would give a much better notch shape. Returning to the optics of the original system would result in an impractically long optical train, especially at the 512 nm wavelength.

The TIR spatial light modulators performed well. As shown with the multiple notch tests, they were extremely effective at blocking a given band of frequencies. Their only drawback is that the individual pixels must be switched every few minutes to avoid damage to the liquid crystal.

5. References:

1. Harris Corporation, Pre-Sort Processor, Final Technical Report, RADC-TR-88-247, October 1988

2. Meadows, M.R., Handschy, M.A., Electro-optic switching using total internal reflection by a ferroelectric liquid crystal, Appl. Phys. Lett., 54(15), April 10, 1989.

3. Meadows, M.R., Handschy, M.A., Electro-optic switching using total internal reflection by a ferroelectric liquid crystal, Appl. Phys. Lett., 54(15), April 10, 1989.

4. Griffiths,D.J., Introduction to Electrodynamics, Prentice Hall, pp. 363-365,1981.

5. Meadows, M.R., Handschy, M.A., Electro-optic switching using total internal reflection by a ferroelectric liquid crystal, Appl. Phys. Lett., 54(15), April 10, 1989.

Appendix A: Equipment List:

laser			
	Adlas	DPY 315 II	diode laser pumped Nd:YAG laser
collimator			
C1	Spindler & Hoyer	06-3120	positive achromat, 16 mm focal length, 7 mm diameter
C2	Spindler & Hoyer	06-3058	bi-concave lens, -20 mm focal length, 21.4 mm diameter
C3	Spindler & Hoyer	06-3422	cylindrical lens, 40 mm focal length, 17 mm by 5 mm
C4	Oriel	43885	cylindrical lens, 150 mm focal length, 1" diameter
interferometer			
BS1	Newport	10BC16NP.3	non-polarizing beam splitter cube, 1" on a side
I1	Oriel	43845	cylindrical lens, 75 mm focal length
BC	Brimrose	TED-35-20	acoustooptic deflector, SN: 9309-AO-326
BS2	Newport	10BC16NP.3	non-polarizing beam splitter cube, 1" on a side
transform optics			
F1	Spindler & Hoyer	06-3223	positive achromat, 160 mm focal length, 30 mm diameter
F2	Oriel	43845	cylindrical lens, 75 mm focal length
F3	Spindler & Hoyer	06-3058	bi-concave lens, -20 mm focal length, 21.4 mm diameter
F4	Melles-Griot	01-LAO-138	positive achromat, 120 mm focal length, 40 mm diameter
spatial light modulator			
	DislayTech Inc.	TIR-200B	SN: 212501
collection optics			
C1	unknown	4636780G01	50 mm focal length, multi-element collection lens
photo receiver			
	Harris Corporation		part of the processor built by Harris Corporation

All mirrors are Spindler & Hoyer(34-0482) dielectric mirrors, for use at 512 nm.

Appendix B: Mechanical Drawings

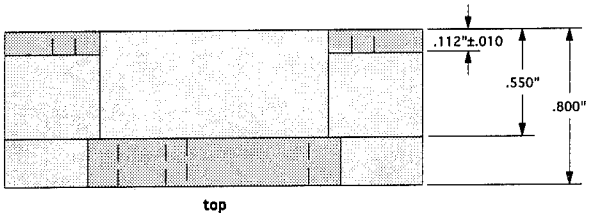

top

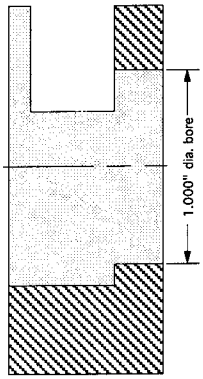

side

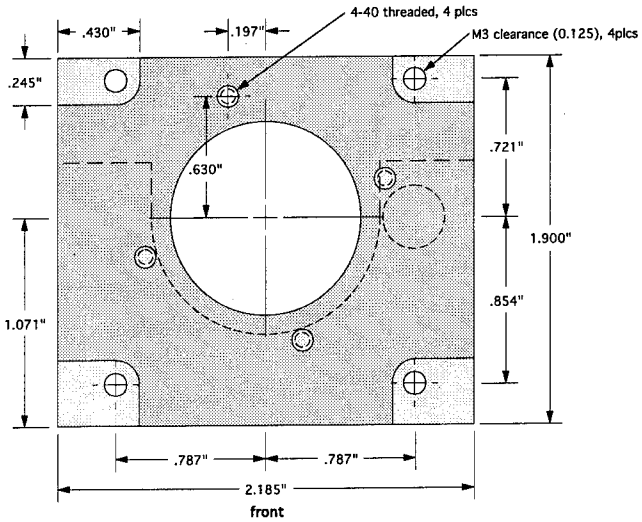

front

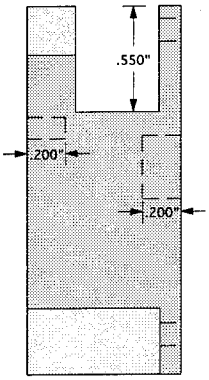

side

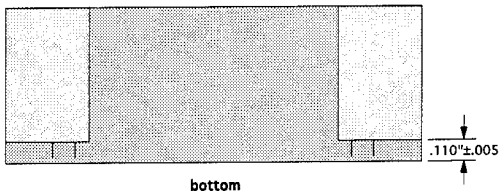

bottom

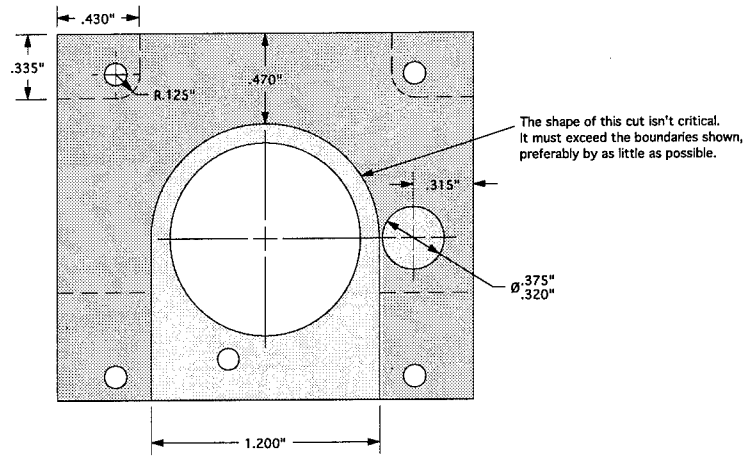

back

Scale 1:1
Material: aluminum
Number of Pieces: 1

David Grucza 2105/2936
July 28,1993
Title: Laser to S&H Adapter

David Grucza, RL/OCPA, X2105
December 21, 1993
Title: Laser Mount -

scale: 1:1
material: aluminum
quantity: two

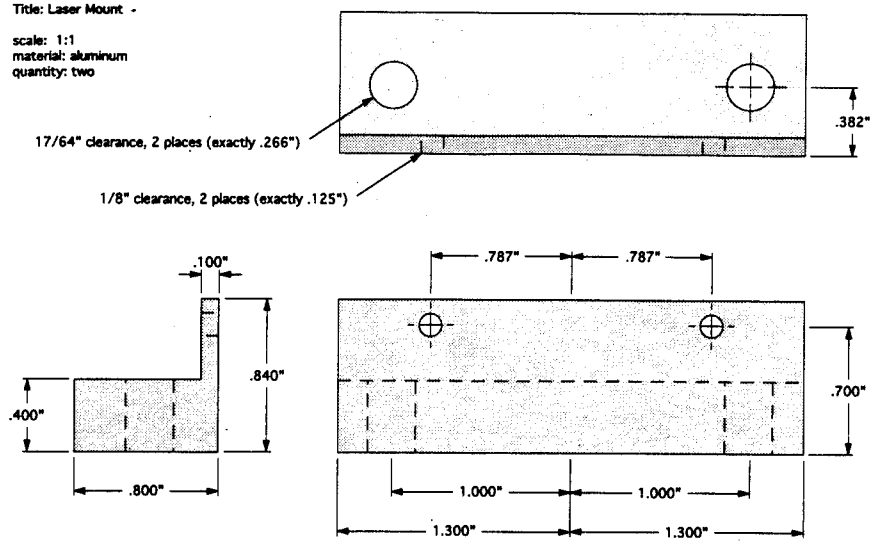

Scale 1:1

Engineer: David Grucza, X2105/2936
Date: March 21,1993
Title: Acoustooptic Cell Mount

scale: 1:1
material: aluminum
quantity: one

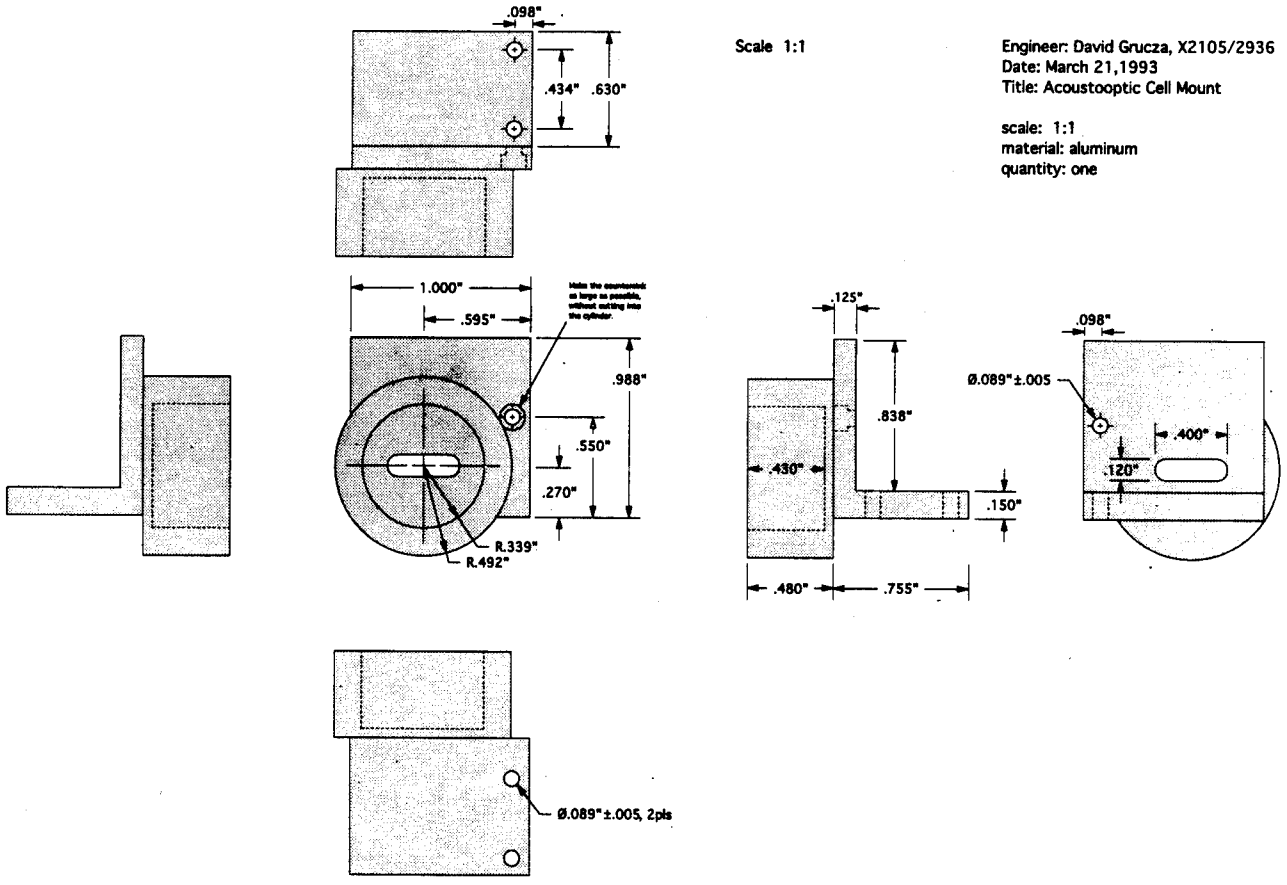

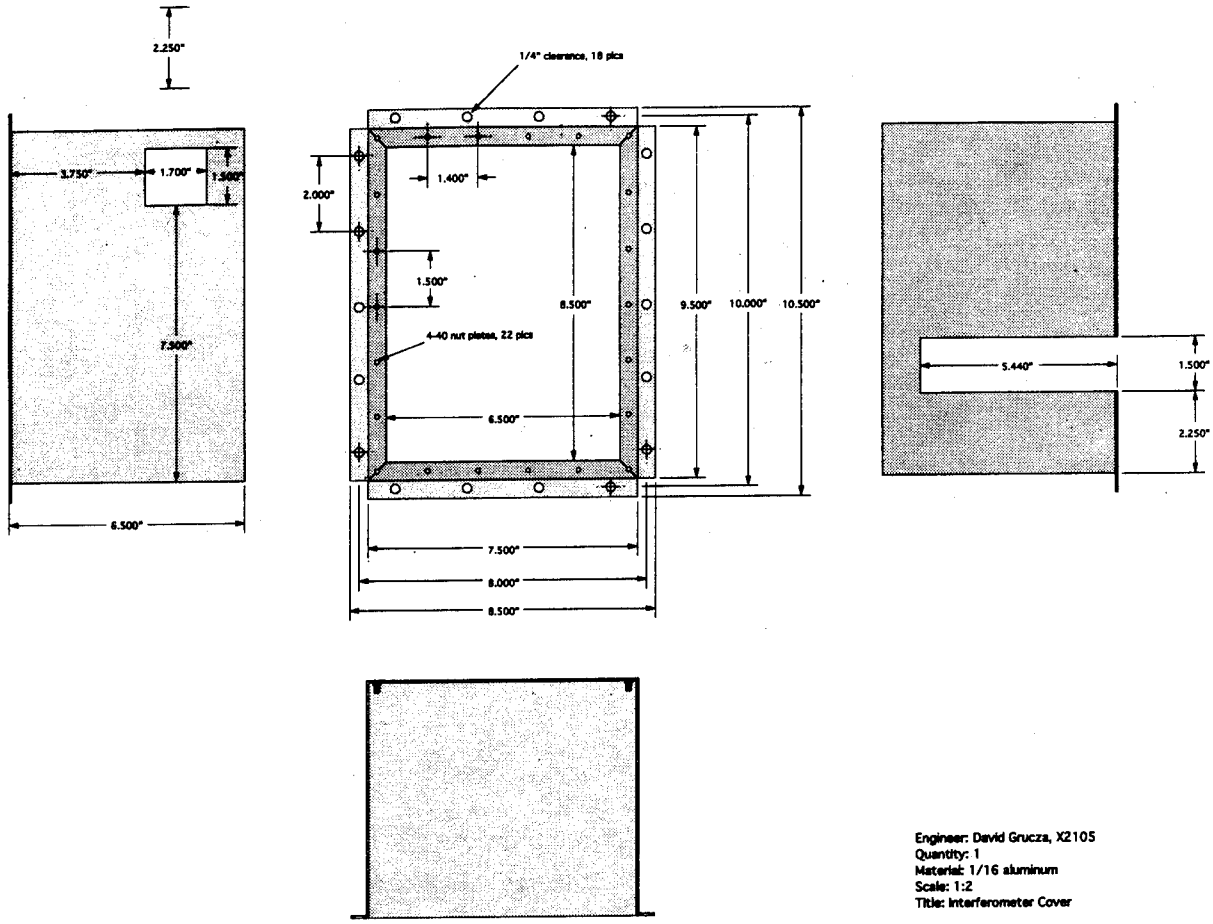

Engineer: David Grucza, X2105
Quantity: 1
Material: 1/16 aluminum
Scale: 1:2
Title: Interferometer Cover

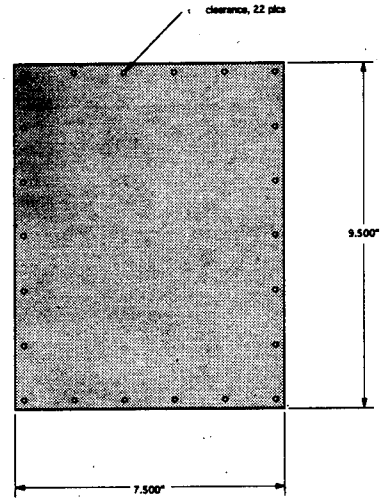

Engineer: David Grucza, X2105
Quantity: 1
Material: 1/16 aluminum
Scale: 1:2
Title: Interferometer Cover Lid

☆U.S. GOVERNMENT PRINTING OFFICE: 1995-610-126-50107

MISSION

OF

ROME LABORATORY

Mission. The mission of Rome Laboratory is to advance the science and technologies of command, control, communications and intelligence and to transition them into systems to meet customer needs. To achieve this, Rome Lab:

a. Conducts vigorous research, development and test programs in all applicable technologies;

b. Transitions technology to current and future systems to improve operational capability, readiness, and supportability;

c. Provides a full range of technical support to Air Force Materiel Command product centers and other Air Force organizations;

d. Promotes transfer of technology to the private sector;

e. Maintains leading edge technological expertise in the areas of surveillance, communications, command and control, intelligence, reliability science, electro-magnetic technology, photonics, signal processing, and computational science.

The thrust areas of technical competence include: Surveillance, Communications, Command and Control, Intelligence, Signal Processing, Computer Science and Technology, Electromagnetic Technology, Photonics and Reliability Sciences.